

Impurity composition and cathodoluminescence of HPHT-diamond type IIb with boron concentration up to 15 ppm

© V.A. Kravets¹, I.V. Klepikov^{2,3}, E.A. Vasilyev⁴

¹ Ioffe Institute,
St. Petersburg, Russia

² LLC NPK „Almaz“,
St. Petersburg, Russia

³ „Diamond Microwave Electronics“ Laboratory of MIREA — Russian Technological University,
Moscow, Russia

⁴ St. Petersburg Mining University,
St. Petersburg, Russia

E-mail: vladislav2033@yandex.ru

Received May 31, 2023

Revised September 3, 2023

Accepted September 6, 2023

A single-crystal multisection plate of HPHT-type IIb diamond by local cathodoluminescence (SL) at 77 K and IR spectroscopy has been studied. The SL features of growth sectors (100), (110), (113), (111) of HPHT-grown diamond were investigated. In the luminescence of the band with a maximum of 2.3 eV, two growth sector species-dependent components with lifetimes in the ranges of 6–13 and 75–115 μ s are identified, respectively. The lifetime of the band with a maximum of 3.0 eV is less than 100 ns. An assumption is made that each growth facet represents a separate luminescent material with its characteristic cathodoluminescent properties. A diagram of boron impurity capture by different growth facets under low-nitrogen growth conditions is constructed.

Keywords: IK spectroscopy, growth sector, luminescence properties, lifetimes.

DOI: 10.61011/PSS.2023.11.57326.99

1. Introduction

Type IIb diamond is a semiconductor with a band gap of 5.5 eV and an acceptor level of 0.37 eV of the boron atom that replaces carbon. As the boron concentration increases, an impurity band is formed with a lower boundary of about 0.12 eV [1]. Natural and synthetic diamonds contain in their structure many defect-impurity centers responsible for luminescence [2–5]. All types of diamonds, when excited by quanta with an energy of more than 5.5 eV, also demonstrate a wide structureless „band A“ in the region of 2.3–3.2 eV [2,6,7]. The nature of the band A luminescence has not been fully clarified to date. This energy range is likely to have an overlap of bands of different origins. Perhaps the band A is due to the recombination of electrons and holes on donor–acceptor (DA) pairs [2,6,7]. The model of the luminescence center proposed in [2,6,7] discusses a nitrogen dimer as the donor and a substitutional boron atom as the acceptor. According to other models, this band is associated with intrinsic defects in the crystalline structure of diamond [8,9,10], in particular, with the sp^2 -hybridization of electron orbitals on dislocations and stacking faults of carbon atoms [6,7]. The luminescence of type IIb diamonds has been repeatedly studied, and its recombination nature is now recognized. As shown in [2,6,7], the luminescent characteristics of the band should depend on the concentration of the doping impurity (boron and nitrogen), however, systematic studies are complicated by the difficulty

of controlling the defect-impurity composition of natural and synthetic diamonds.

Modern methods of diamond synthesis make it possible to control the presence and concentration of doping impurities in the process of growth. There are two main competing methods for growing diamonds: high-pressure high temperature (HPHT) method and chemical vapor deposition (CVD). Previously, high boron concentrations were achieved in both CVD and HPHT diamonds, but the CVD method currently has advantages due to the layer-by-layer deposition of diamond. In this study, data was obtained on the spectral-time characteristics of luminescence in different growth sectors of a type IIb diamond single crystal with a boron concentration of up to 15 ppm, grown by the HPHT method.

2. Sample

A blue multi-sector $\sim 7.5 \times 3.0 \times 0.5$ mm wafer of type IIb HPHT-diamond was studied. This wafer was cut using laser cutting technology perpendicular to the $\langle 111 \rangle$ direction from the central part of a type IIb HPHT-diamond single crystal, and then mechanically polished using a polishing disk. The crystal morphology was dominated by the $\{111\}$ facets, but $\{100\}$, $\{110\}$, $\{113\}$, $\{115\}$ facets were present as well. The crystals were synthesized in a SK-850 high-pressure cubic press in a temperature

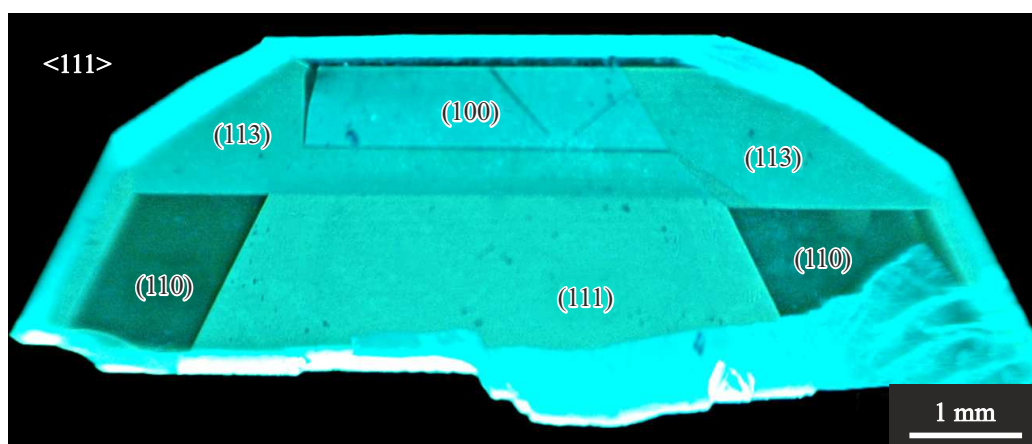


Figure 1. Photoluminescent microscopy image of the sectorial internal structure of a diamond wafer (with excitation at $\lambda = 220$ nm).

range of 1450–1550°C, at a pressure of 5.5 GPa. Boron was added to the carbon source, and a Fe-Co alloy was used as a catalyst metal with the addition of Ti, Al as nitrogen recipients. In the high-pressure cell, 4 {111} facet oriented seeds were placed.

3. Research methods

The content of nitrogen and boron impurities was assessed using IR absorption spectra. Absorption spectra were recorded on a Bruker Vertex-70 spectrometer with a Hyperion 1000 microscope in a range of 600–6000 cm^{-1} with a resolution of 2 cm^{-1} , with averaging over 32 scans with a recording area size of 100 × 100 μm .

The boron concentration was determined using known relationships [11–15]:

$$[\text{B}](\text{ppm}) = (5.53 \cdot 10^{-4})I_{2802} \text{ cm}^{-2}, \quad (1)$$

$$[\text{B}](\text{ppm}) = (5.53 \cdot 10^{-4})I_{2450} \text{ cm}^{-2}, \quad (2)$$

where I_{2450} and I_{2802} are integral absorption coefficients of the corresponding bands.

The sectorial structure of the diamond wafer was visualized using photoluminescent microscopy using a Diamond Inspector instrument with an excitation wavelength of 220 nm. Cathodoluminescence (CL) spectra were recorded by a CAMEBAX electron probe microanalyzer (Cameca, France) equipped with an optical microscope and combined with an originally-designed cathodoluminescence station [16]. The CAMEBAX microanalyzer allows recording optical images of a sample in reflected light, measuring life time and rise time of the luminescence at a CL-station with a time resolution of 100 ns, and recording spectra (CL) with a spatial resolution of 1 μm . The CL spectra were recorded with an accelerating voltage of 15 kV, a current of 20 nA absorbed by the sample, and an electron beam diameter of 3 μm at 77 K.

4. Results and discussion

4.1. The luminescent microscopy

Figure 1 shows luminescent microscopy images of the sample. The images show a contrast typical for HPHT-diamonds. Based on the morphology of the crystal and the arrangement of growth pyramids of facets of simple shapes, (100), (111), (110), and (113) growth sectors were identified.

4.2. IR absorption spectra

Figure 2 shows the IR absorption spectra recorded in different growth sectors of the diamond wafer. These spectra demonstrate bands at 1290, 2360, 2450, 2800, 3740, 4080, 5025, 5025, and 5370 cm^{-1} , that characterize the presence of boron impurity in the crystal [12]. Also, an absorption band with a maximum at 1290 cm^{-1} can be seen, which

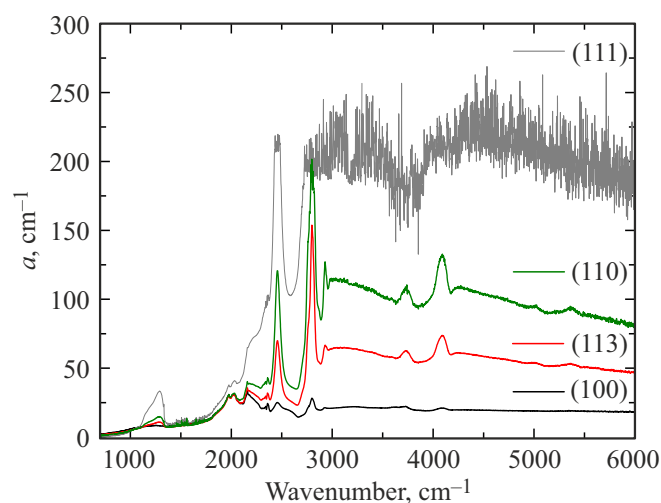


Figure 2. IR absorption spectra of various growth sectors of type IIb HPHT-diamond.

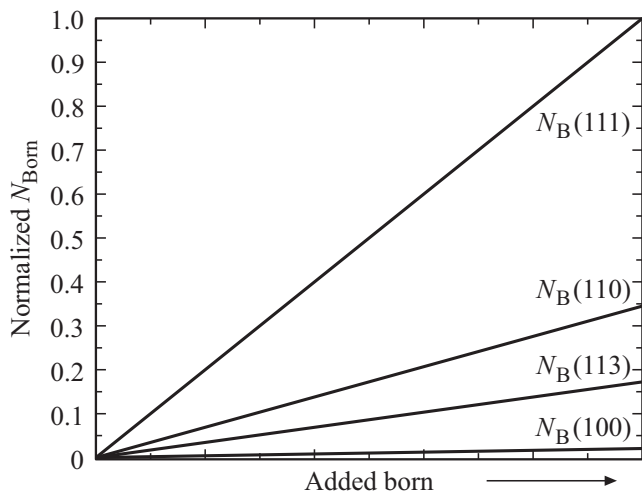


Figure 3. Diagram of boron content in different growth sectors under low nitrogen synthesis conditions.

outline is typical for type IIb diamond. The intensity of this band is high only for the (111) sector. The high noise level in the absorption spectrum for the (111) sector is explained by the low transmittance of this region (close to the sensitivity limit of the instrument).

The boron concentration was calculated using the most intense bands with maxima at 2450 and 2800 cm^{-1} . Results are shown in Table 1. As the boron concentration in diamond increases, the transmittance decreases. In the case of low concentration, the accuracy of determining the boron concentration is higher in the 2800 cm^{-1} band. It is also worth noting that there are no bands in the IR spectra associated with the impurity of single nitrogen at the substitution position or with the ionized state of this center [12]. Thus, no nitrogen content in the sample was detected at the level of the detection limit ($< 0.5\text{ ppm}$) or below it. It is known that there is a significant difference in the distribution of nitrogen across sectors in type Ib diamonds, which can be very strong [17]. In this study, the nitrogen ratio of $1:10:46:100$ was obtained for the sectors of $(110):(113):(100):(111)$, respectively.

Based on the calculated boron concentrations, Figure 3 shows a modified diagram of boron content in various growth sectors. The results for the studied sample correlate with the data for previously studied crystal with a different boron content [18].

4.3. CL-studies

CL spectra of the identified growth sectors of the sample are presented in Figure 4. The shape of the

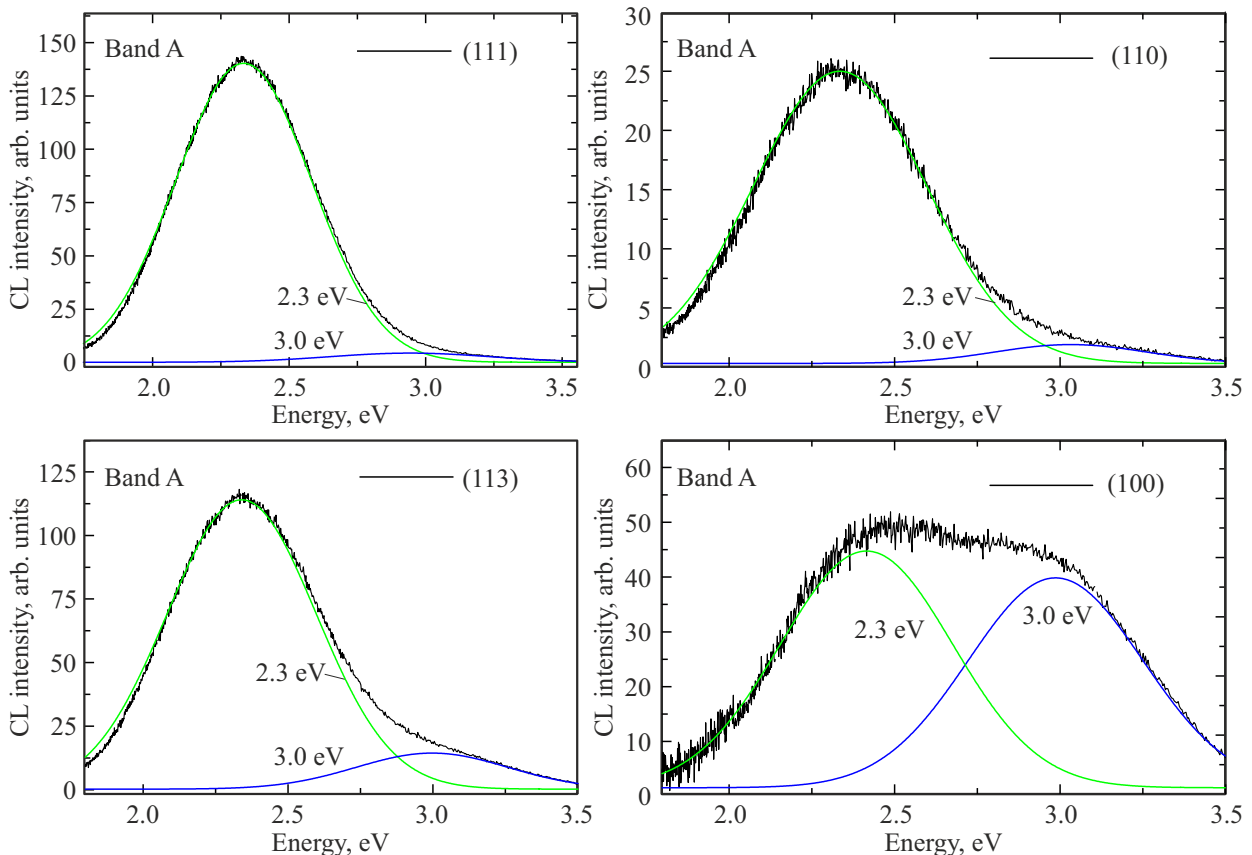


Figure 4. CL spectra of the sample at 77 K, recorded from different areas of the sample.

Table 1. Concentrations of boron and nitrogen in different sectors of the diamond

Sector	B, ppm (2450 cm ⁻¹)	B, ppm (2800 cm ⁻¹)	N, ppm (not detected)
[111]	14.4 ± 1.5	–	< 0.5
[110]	5.2 ± 0.5	4.8 ± 0.5	< 0.5
[113]	2.7 ± 0.5	2.2 ± 0.5	< 0.5
[100]	0.4 ± 0.1	0.2 ± 0.1	< 0.5

Table 2. Time characteristics of band A

Sector	Life time of luminescence band, 2.3 eV		Life time of luminescence band, 3.0 eV
	<i>t</i> ₁ , μs	<i>t</i> ₂ , μs	<i>t</i> ₁ , ns
	(111)	111 ± 4	13 ± 1
(110)	76 ± 3	6 ± 1	< 100
(113)	75 ± 3	6 ± 1	< 100
(100)	83 ± 3	6 ± 1	< 100

spectra for each sector corresponds to the superposition of the band A observed in all diamonds, and a wide structureless band with a maximum of 2.3 eV. The most intense luminescence of the 2.3 eV band is observed in the ⟨111⟩ sector. The intensity of the band does not depend directly on the boron content. The relative intensity of the band with a maximum of 3.0 eV increases with decreasing boron concentration.

The luminescence life times of the bands with maxima of 2.3 and 3.0 eV are presented in Table 2 and correspond to the literature data of the band A time analysis [19]. And no correlation is observed between luminescence life times and boron concentration.

It can be seen from the data obtained that each sector is a separate luminescent material with its own characteristic luminescent properties. The recombination model of luminescence assumes [6,19] the existence of a dependence of the position of luminescence band maximum on the concentration of the donor and acceptor

$$E(r) = E_g - (E_{ac} - E_d) + e^2/\epsilon r,$$

where $E(r)$ is photon energy, E_g, E_{ac}, E_d is band gap and position of the acceptor and donor levels, respectively, e is electron charge, ϵ is dielectric constant, r is distance between donor and acceptor. At this stage of research, no shift in the maximum of the 2.3 and 3.0 eV band in sectors with different boron concentrations was noticed.

Apparently, each sector has its own ratio of boron and nitrogen, and, accordingly, its own set of defects in the crystal structure and the ratio of donor-acceptor pairs. To determine the nature of the 2.3 and 3.0 eV bands, it is necessary to study the luminescence characteristics

in samples with reliably controlled concentrations of both boron and nitrogen.

5. Conclusion

This study shows that the luminescent properties of HPHT-diamond growth facets weakly correlate with the boron content. Each growth facet is a separate luminescent material with its own characteristic cathodoluminescent properties. Thus, it is necessary to compare the properties of certain growth sectors to each other, and not the entire diamond as a whole.

Funding

The results of the study regarding the analysis of growth sectors, luminescence distribution with excitation at 220 nm and the interpretation of these data were obtained by I.V. Klepikov within the work under the state assignment of the Ministry of Science and Higher Education of the Russian Federation (topic No. FSFZ-2022-0006).

Conflict of interest

The authors declare that they have no conflict of interest.

References

- [1] G.T. Williams, J.A. Calvo, F. Dodson, T. Obeloer, D.J. Twitchen, 17th IEEE Intersociety Conference on Thermal and Thermomechanical Phenomena in Electronic Systems (ITherm). San Diego, USA, 235–239 (2018).
- [2] T. Shao, F. Lyu, X. Guo, J. Zhang, H. Zhang, X. Hu, A.H. Shen. Carbon **167**, 888 (2020).
- [3] A.T. Collins, E.C. Lightowers, J.E. Field. The properties of diamond. Academic Press, London, UK (1979).
- [4] A.T. Collins. Semicond. Sci. Technol. **4**, 8, 605 (1989).
- [5] J. Walker. Rep. Prog. Phys. **42**, 10, 1605 (1979).
- [6] P.J. Dean. Phys. Rev. **139**, 2A, 588 (1965).
- [7] H. Kawarada, Y. Yokota, Y. Mori, K. Nishimura, A. Hiraki. J. Appl. Phys. **67**, 2, 983 (1990).
- [8] I. Kiflawi, A.R. Lang. Phil. Mag. **30**, 1, 219 (1974).
- [9] S.J. Pennycook, L.M. Brown, A.J. Craven. Phil. Mag. A **41**, 4, 589 (1980).
- [10] N. Yamamoto, J.C.H. Spence, D. Fathy. Phil. Mag. B **49**, 6, 609 (1984).
- [11] A.T. Collins, A.W.S. Williams. J. Phys. C **4**, 13, 1789 (1971).
- [12] B. Dishler. Handbook of Spectral Lines in Diamond. Springer (2012). 467 p.
- [13] D. Fisher, S.J. Sibley, C.J. Kelly. J. Phys.: Condens. Matter **21**, 36, 364213 (2009).
- [14] S. Karna, D.V. Martyshkin, Y.K. Vohra, S.T. Weir. MRS Proc. **1519**, 1, 327 (2013).
<https://link.springer.com/article/10.1557/opl.2012.1759>
- [15] G. Davies, P.L. Walker, P.A. Throer. In: Chemistry and Physics of Carbon / Eds P.L. Walker Jr, P.A. Throer. Dekker, N.Y. (1977). P. 34.

- [16] M.V. Zamoryanskaya, S.G. Konnikov, A.N. Zamoryanskii. Instrum. Exp. Tech. **47**, 4, 477 (2004).
- [17] R. Burns, V. Cvetkovic, C.N. Dodge, D.J.F. Evans, M.-L.T. Rooney, P. Spear, C. Welbourn. J. Crystal Growth **104**, 2, 257 (1990).
- [18] I.V. Klepikov, A.V. Koliadin, E.A. Vasilev. IOP Conf. Ser. **286**, 1, 012035 (2017).
- [19] P.B. Klein, M.D. Crossfield, J.A. Freitas Jr, A.T. Collins. Phys. Rev. B **51**, 15, 9634 (1995).

Translated by Y.Alekseev